Video Article

Fabrication of Mechanically Tunable and Bioactive Metal Scaffolds for Biomedical Applications

Hyun-Do Jung[1], Hyun Lee[2], Hyoun-Ee Kim[2,3], Young-Hag Koh[4], Juha Song[3]

[1]Liquid Processing & Casting Technology R&D Group, Korea Institute of Industrial Technology

[2]Department of Materials Science and Engineering, Seoul National University

[3]Advanced Institutes of Convergence Technology, Seoul National University

[4]School of Biomedical Engineering, Korea University

Correspondence to: Juha Song at sat105@snu.ac.kr

URL: https://www.jove.com/video/53279
DOI: doi:10.3791/53279

Keywords: Bioengineering, Issue 106, Porous metal scaffold, titanium, sustainable drug release, hard tissue engineering, functionally graded materials, freeze casting

Date Published: 12/8/2015

Citation: Jung, H.D., Lee, H., Kim, H.E., Koh, Y.H., Song, J. Fabrication of Mechanically Tunable and Bioactive Metal Scaffolds for Biomedical Applications. *J. Vis. Exp.* (106), e53279, doi:10.3791/53279 (2015).

Abstract

Biometal systems have been widely used for biomedical applications, in particular, as load-bearing materials. However, major challenges are high stiffness and low bioactivity of metals. In this study, we have developed a new method towards fabricating a new type of bioactive and mechanically reliable porous metal scaffolds-densified porous Ti scaffolds. The method consists of two fabrication processes, 1) the fabrication of porous Ti scaffolds by dynamic freeze casting, and 2) coating and densification of the porous scaffolds. The dynamic freeze casting method to fabricate porous Ti scaffolds allowed the densification of porous scaffolds by minimizing the chemical contamination and structural defects. The densification process is distinctive for three reasons. First, the densification process is simple, because it requires a control of only one parameter (degree of densification). Second, it is effective, as it achieves mechanical enhancement and sustainable release of biomolecules from porous scaffolds. Third, it has broad applications, as it is also applicable to the fabrication of functionally graded porous scaffolds by spatially varied strain during densification.

Video Link

The video component of this article can be found at https://www.jove.com/video/53279/

Introduction

While metallic biomaterials have been widely used as load-bearing implants and internal fixation devices because of their excellent mechanical strength and resilience,[1-3] they involve two critical challenges: 1) mechanical mismatch because metals are much stiffer than biological tissues, causing undesirable damages to the surrounding tissues and 2) low bioactivity that often results in poor interface with biological tissues, often provoking foreign body reactions (*e.g.,* inflammation or thrombosis).[4-6] Porous metallic scaffolds have been proposed to promote bone ingrowth in the structures, improving bone-implant contact while the stress shield effects are suppressed because of their reduced stiffness.[7-9] Moreover, various surface modifications have been applied to enhance the biological activities of metallic implants; such modifications include coating the metal surface with bioactive molecules (*e.g.*, growth factors) or drugs (*e.g.*, vancomycin, tetracycline).[10-12] However, problems such as reduced mechanical properties of porous metal scaffolds, decreased stiffness and the fast release of the bioactive coating layers remain unresolved.[13-16]

In particular, titanium (Ti) and Ti alloys are one of the most popular biometal systems because of their excellent mechanical properties, chemical stability, and good biocompatibility.[13,17-19] Their foam-shaped applications have also attracted increasing interest because the 3D porous networks promote bone ingrowth in addition to bone-like mechanical properties.[20-22] Efforts have been made to improve the mechanical properties by developing new manufacturing techniques including replication of polymeric sponge, sintering of metal particles, rapid prototyping (RP) method, and space holder method in order to control the various features of the pores (*e.g.*, pore fraction, shape, size, distribution, and connectivity) and material properties (*e.g.*, metallic phase and impurity).[23-25] Recently, the freeze casting of water-based metal slurry has gained considerable attention to produce mechanically enhanced Ti forms with well-aligned pore structures by utilizing the unidirectional ice dendrite growth during solidification; however, oxygen contamination caused by contact of metal powders with water requires special care to minimize the embrittlement of Ti scaffolds.[14,15]

Therefore, we have developed a new approach towards fabricating bioactive and mechanically tunable porous Ti scaffolds.[25] The scaffolds initially have porous structures with a porosity of more than 50%. The fabricated porous scaffolds were coated with bioactive molecules and then compressed using a mechanical press during which the final porosity, mechanical properties and drug release behavior were controlled by the applied strain. The densified porous Ti implants have shown low porosity with good strength in spite of the low stiffness comparable to that of bone (3-20 GPa).[2] Because of the coating layer, the bioactivity of the densified porous Ti was significantly improved. Moreover, because of the

unique flat pore structures induced by the densification process, the coated bioactive molecules were seen to be gradually released from the scaffold, maintaining their efficacy for a prolonged period.

In this study, we introduced our established method to fabricate densified porous Ti scaffolds for potential use in biomedical applications. The protocol includes dynamic freezing casting with metal slurries and densification of porous scaffolds. First, to fabricate porous Ti scaffolds with good ductility the dynamic freeze casting method was introduced as shown in **Figure 1A**. Ti powder was dispersed in liquid camphene; then, by decreasing the temperature, the liquid phase was solidified, resulting in the phase separation between the Ti powder network and solid camphene crystals. Subsequently, the solidified Ti-camphene green body was sintered in which Ti powders were condensed with continuous Ti struts, and the camphene phase was completely removed to obtain a porous structure. The coating and densification process with the obtained porous scaffolds was employed, varying the degree of densification and initial porosity. The coating layer and its release behavior were visualized and quantified using the green fluorescent protein (GFP)-coated porous Ti with and without densification compared to the GFP-coated dense Ti. Finally, functionally graded Ti scaffolds that have two different porous structures were proposed and demonstrated by varying the degree of densification of the inner and outer parts of the porous scaffolds.

Protocol

1. Fabrication of Porous Metal Scaffolds

1. Prepare Ti-camphene slurries by mixing commercially available Ti powder, camphene, and KD-4 after weighing the appropriate amounts of materials as described in **Table 1** for porous Ti scaffolds with four initial porosities (40, 50, 60, and 70). Pour the slurries into 500 ml polyethylene (PE) bottles and rotate the bottles at 55 °C for 30 min in a ball-mill oven at 30 rpm.
2. Pour the slurries from the PE bottles into cylindrical aluminum (Al) molds with a diameter of 60 mm and a height of 60 mm. Seal each Al mold with the corresponding Al cover slip and rotate the molds in a ball-mill oven at a speed of 30 rpm at 55 °C for 10 min.
    1. Subsequently, decrease the temperature of the ball-mill oven to 44 °C, and continuously rotate the molds at a speed of 30 rpm at the constant temperature of 44 °C for 12 hr.
3. Take out the mold from the ball-mill oven after additionally rotating the molds at RT for 1 hr for the cooling process. Remove the solidified titanium/camphene green body from the Al mold using an Al plunger.
4. Place the solidified titanium/camphene green body in a rubber bag by hand and completely seal the rubber bag by tying the mouth of the bag with a string. Place the rubber bag in the water tank of a cold isostatic pressing (CIP) machine and apply an isostatic pressure of 200 MPa for 10 min. Remove the compressed green body from the rubber bag.
5. Transfer the Ti-camphene green body on to an alumina crucible by hand and place the crucible in the freeze-dryer machine. Freeze-dry the green body to sublimate the camphene phase in the green body at - 40 °C for 24 hr.
6. Subsequently, close the crucible with an alumina cover slip and place the closed crucible in a vacuum furnace (below 10^{-6} Torr) at RT. Then, increase the temperature of the furnace to 1,300 °C at a heating rate of 5 °C/min and hold the temperature at 1,300 °C for 2 hr.
7. After the heat treatment, keep the sintered porous Ti in the furnace for 6-7 hr until the furnace is fully cooled to RT.
   Note: During 6 hr of the cooling process, the average cooling rate of the furnace above 400 °C is ~15 °C/min and the average cooling rate of the furnace below 400 °C is ~2 °C/min.
8. If necessary, cut the block of sintered porous Ti into disc-shaped samples with a diameter of 16 mm through electrical discharge machining (EDM).[27]
   Note: Depending on the size of the Al molds, the size of the sintered porous Ti needs to be modified through the machining process (**Figure 2A**).
9. Place a glass beaker with the porous Ti samples in an autoclave and sterilize the samples at 121 °C for 15 min. Remove the samples from the autoclave. Wash the porous Ti samples with distilled water twice and then with 70% ethanol twice. Finally, leave the porous Ti into a Petri dish and air-dry the samples at RT on a clean bench under UV light.

2. Dip Coating of Scaffolds with Bioactive Agents

1. Dilute the commercial Green Fluorescence Protein (GFP) from 1 mg/ml to 100 µg/ml in a clean bench by mixing 1 ml of GFP with 9 ml of Dulbecco's Phosphate Buffered Saline (DPBS, pH 7.4) solution in a 10 ml-sterilized polystyrene (PS) tube as indicated in **Table 1**.
2. Immerse the sterilized dense or porous Ti in 10 ml of diluted GFP solution (100 µg/ml) by placing the Ti samples into the PS tube with the GFP solution at RT and placing on a clean bench.
3. Place the PS tube in a vacuum desiccator and evacuate the desiccator for 10 min to ensure the GFP solution penetrates the pores of the porous Ti more effectively.
4. Remove the porous titanium from the PS tube using tweezers. Place the GFP-coated porous Ti into a 10 cm diameter Petri dish and air-dry O/N at RT on a clean bench.
5. Rinse the porous Ti twice with 10 ml of Dulbecco's Phosphate Buffered Saline (DPBS) in a glass beaker, and move the porous Ti into a 10 cm diameter Petri dish using tweezers and air-dry at RT on a clean bench.

3. Densification of Porous Scaffolds

1. Place the GFP-coated porous Ti samples with various heights in a cylindrical steel die, and insert a set of punches into the top and bottom holes of the steel die (**Figure 3A**).
2. Compress the porous Ti within the steel die assembly at RT in the z direction of the sample (**Figure 3A**) using a press machine at intermediate strain rates of 0.05 ~ 0.1 sec^{-1} against the predetermined applied strains shown in **Table 2**. Hold the pressure for 1 min before unloading.

3. Remove the densified Ti samples from the steel die. Wash the densified samples twice with 10 ml of DPBS in a beaker and air-dry O/N at RT on a clean bench.

4. Release Test of GFP-coated Scaffolds

1. Immerse three types of specimens (GFP-coated dense Ti (after steps 2), GFP-coated porous Ti (after steps 1 and 2) and GFP-coated densified porous Ti (after steps 1-3)) in 5 ml DPBS (pH 7.4) solution contained in a 10 ml sterilized PS tube at 37 °C on a clean bench.
2. Suction out all the DPBS solution from each PS tube with the GFP-coated sample and replenish with a new 5 ml DPBS solution (pH 7.4) using a pipette according to the predetermined times of 1, 2, 3, 5, 8, 12, 15, 22 and 29 days after immersion.
3. Take the fluorescence images of the GFP-coated samples before immersion (day 0) and after 22 day-immersion using confocal laser scanning spectroscopy (CLSM).
4. Measure the fluorescence signal intensity of the released GFP in 1 ml solution from a total of 5 ml DPBS solution drawn from each PS tube in section 4.2 using UV spectroscopy at a wavelength of 215 nm. Convert the intensity value into the concentration of the GFP solution using the standard curve.
   Note: Before the measurement, draw the standard curve of GFP solution by measuring the fluorescence signal intensity of the GFP solution in the concentration range of 0 ng/ml - 10 µg/ml.

5. Fabrication of Graded Porous Ti Scaffolds

1. Produce a block of the sintered porous Ti by repeating step 1.1 to step 1.7.
2. Machine the sintered porous Ti block according to the predetermined structure designs (*e.g.*, **Figure 5a** and **5d**) by EDM.
3. Place the machined Ti samples with height distribution in a steel die where the diameter of porous Ti is ~0.1 mm smaller than the diameter of the die and insert a set of punches into the top and bottom holes of the steel die.
4. Perform steps 3.2 and 3.3.

6. Porosity Measurement of Ti Scaffolds

1. Measure the mass (m_s) of Ti scaffolds.
2. Calculate the apparent volume (V_s) by measuring length, width and height of Ti scaffolds.
3. Compute the porosity using the following equation:

$$P = 100\left(1 - \frac{m_S/V_S}{\rho_{Ti}}\right).$$

where P is the total porosity percentage, ρ_{Ti} is the theoretical density of the titanium and m_S/V_S is the measured density of the sample.
Note: The porosity of Ti samples can be directly retrieved from microCT images after microCT imaging is carried out using a micro-computed tomography scanner.

Representative Results

The fabrication process used to produce porous Ti scaffolds is illustrated in **Figure 1A**. Ti powder is kept dispersed homogeneously in camphene by continuous rotation of the container at 44 °C for 12 hr and, while liquid camphene is fully solidified, any sediments of relatively heavy Ti powder can be minimized. As a result, the homogeneous Ti-camphene green body was produced using the dynamic freeze casting process as shown in **Figure 1B,** in which 3-dimensionally interconnected large camphene pores are surrounded by the Ti powder phase (**Figure 1C**). However, the incorrect rotation of the containers often results in inhomogeneous distribution of Ti and camphene phases in the green body, causing distortion or cracking of the porous scaffold following heat treatment. The optimal condition of the rotation speed was found to be 30 rpm, which was able to produce a homogeneous green body in most cases. Before proceeding with heat treatment, the extensive growth of camphene is confirmed by observing the cross-section of the Ti-camphene green body as shown in **Figure 1C**. If the camphene phase is discontinuous with a significant size distribution of pores, the temperature and time of the dynamic freeze casting needs to be reset. Typically, the camphene phase of the Ti-camphene green bodies was found to be well-developed after 12 hr dynamic freeze casting, where the camphene phase became continuous since large spherical pores were in contact with each other. The size, morphology and connectivity of pores in porous Ti were further evaluated using micro-CT analysis after heat treatment.

After sintering at 1,300 °C, the porous Ti blocks are cut into multiple cylindrical-shaped samples by electrical discharge machining (**Figure 2A**). The obtained cylindrical specimens did not show cracks or defects. Representative micro-CT images of the porous Ti scaffolds fabricated by conventional (top) and dynamic freeze casting (bottom) are shown in **Figure 2B**. The pore structure of the Ti samples from the conventional freeze casting shows directional pore alignment with irregularly shaped pores because of the dendritic growth of camphene during freezing. On the other hand, the sample from dynamic freeze casting exhibits almost spherical pores with random pore distribution. Moreover, the higher resolution microscopic images of the porous Ti scaffolds with various porosities (Initial Porosity (I.P.) = 50, 60, and 70 vol%) clearly show spherical pores randomly distributed within the Ti network (**Figure 2C**). The pore size of the porous Ti scaffolds decreased as the volume of camphene decreased.

Subsequently, the fabricated porous Ti scaffolds are coated with biomolecules and densified within the mold by varying the applied strain as shown in **Figure 3A**. For the visualization of the bioactive coating layer on the Ti samples, green fluorescent protein (GFP) was used in this study. The applied strain (ε_{zz}), which corresponds to the pressure (P_{zz}), is found to vary the degree of densification as shown in **Figure 3B**. The pore shape becomes flattened as the degree of densification increases and, as a result, at the highest densification, pores almost disappear because neighboring pores are in contact with each other. However, from our previous study, we confirmed that the pore channels of the densified samples are still open, with almost the same surface area as that of the porous Ti of the same porosity.[25] To evaluate the densified

samples with different starting porosities, the z-height should vary depending on the initial porosity in order for the densified sample to have the same final porosity. **Table 2** also provides the predicted applied strains to obtain the targeted final porosity (F.P) of the densified porous scaffolds with different initial porosities. For example, to produce the densified porous specimens with F.P. = 5%, the porous scaffold with I.P. = 70% requires a strain of approximately 0.7, while the scaffold with I.P. = 50% needs approximately 0.5. Therefore, the initial heights of the porous scaffolds were carefully calculated according to the initial porosity in order to obtain samples with the same final height after densification. As shown in **Figure 3C**, four specimens with varying porosities from I.P. = 40% to 70% show different initial heights before densification and then at the end, with almost identical heights of 2 mm.

GFP was used to visualize the coating layer on porous (I.P. = 70%) and densified porous Ti (I.P. = 70%, F.P. = 7%) samples compared to commercial dense Ti as shown in **Figure 4A**. All three samples clearly display the coated surface morphology corresponding to their microstructures. The fully dense Ti surface is completely covered with a green coating layer, whereas porous and densified porous samples have green colored Ti struts with clear pores. Using these three coated samples shown in **Figure 4A**, the release behavior was observed (**Figure 4B**). The amount of released GFP from each sample was expressed as the mean ± standard deviation (n=3) and was tracked up to one month by measuring the intensity of fluorescence. Both dense and porous Ti were found to have fast GFP release behavior with initial bursting effect, with most released within one week. However, densified porous Ti shows continuous release up to one month, clearly showing GFP on the surface even after one month (CLSM images of **Figure 4B**).

The densification process can also be applied to the fabrication of functionally graded porous Ti scaffolds as introduced in **Figure 5**. The two potential design schematics of gradient structures were chosen, of which the inner and outer layers of a cylindrical scaffold have different porosities. For the structure with a denser core shown in **Figure 5A**, the outer part of the Ti scaffold was shortened by mechanical machining as shown in **Figure 5B**. After selective densification of the higher inner part, the gradient structure was obtained. The detailed structural information of **Figures 5Bb** and **5E** measured by micro CT is provided in **Table 3**. The micro CT image of **Figure 5C** clearly shows the inner and outer parts of the scaffold with different porosities (inner: F.P. = ~60%, outer: F.P. = ~70%). Alternatively, a structure with denser outer layer can be produced by changing the height difference between the inner and outer parts (**Figure 5D**). The porous Ti with the higher outer and lower inner parts results in a denser outer part after densification (**Figure 5E**), in which the porosity of the outer part was lowered to ~45%, with the inner part having the preserved initial porosity (I.P. = 70%) as indicated in **Figure 5F**.

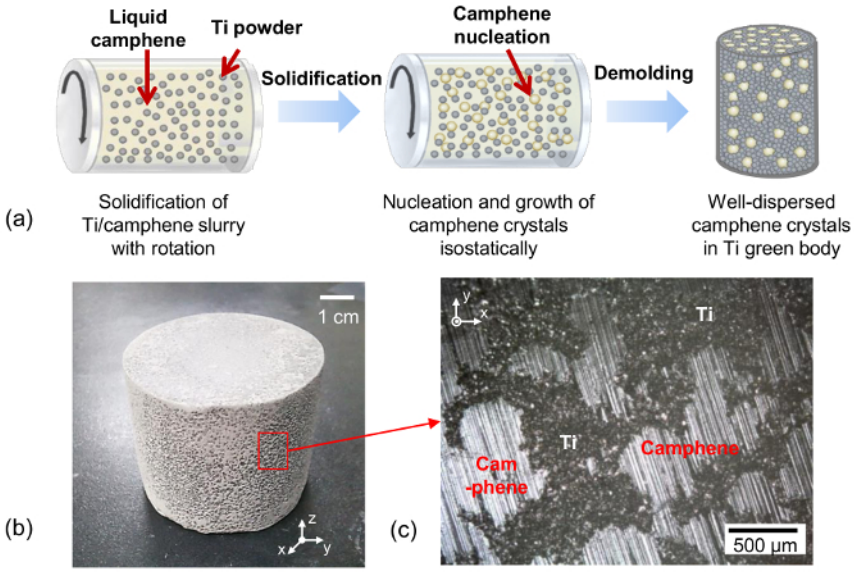

Figure 1. Fabrication of Ti-camphene green body by dynamic freeze casting. (**A**) Schematic illustration of the dynamic freeze casing process to obtain solidified Ti-camphene green body before heat treatment (Adapted with permission from Elsevier, Jung *et al.*, 2013). (**B**) Optical image of a representative Ti-camphene green body after the completion of the dynamic freeze casting process. (**C**) Cross-sectional image of the Ti-camphene green body in which the solid camphene phase is randomly distributed within the continuous Ti powder phase. Please click here to view a larger version of this figure.

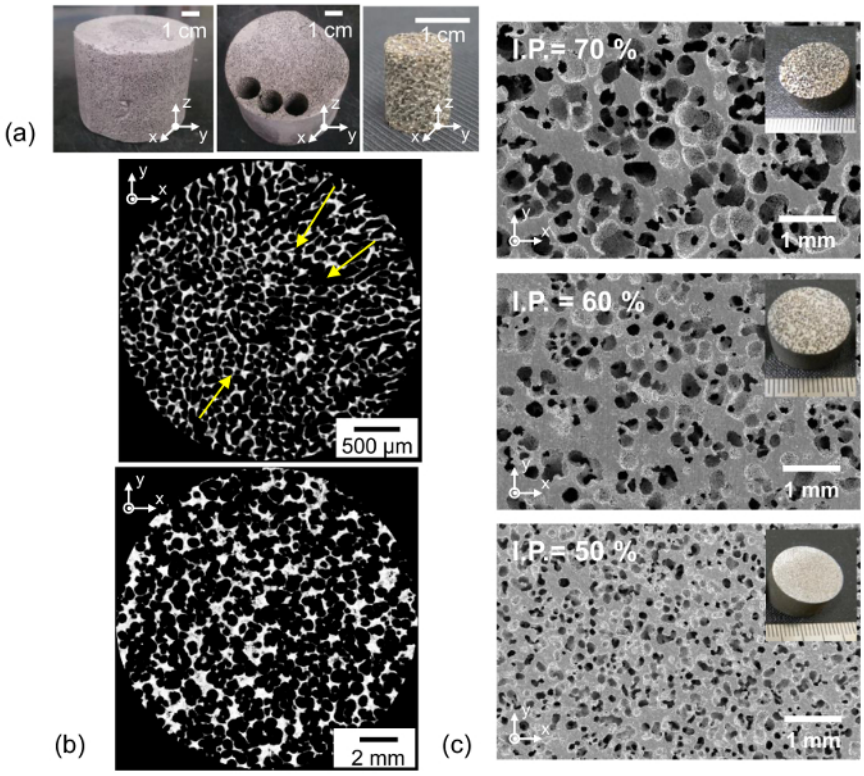

Figure 2. Porous Ti scaffolds with various initial porosities after heat treatment. (**A**) Optical images of a fully sintered porous Ti block before and after machining and an obtained cylindrical porous Ti scaffold from machining. (**B**) Sectional micro-CT images of the porous Ti scaffolds fabricated by conventional freeze casting (top) and dynamic freeze casting (bottom). Yellow arrows on the top image of **Figure 2B** indicate the pore alignment in the radial direction. (**c**) Cross-sectional images of the porous Ti scaffolds fabricated by dynamic freeze casting with the initial porosity (I.P.) of 70% (top), 60% (middle) and 50% (bottom) where insets are the optical images of the corresponding porous Ti scaffolds (Adapted with permission from Elsevier, Jung *et al*., 2013). Please click here to view a larger version of this figure.

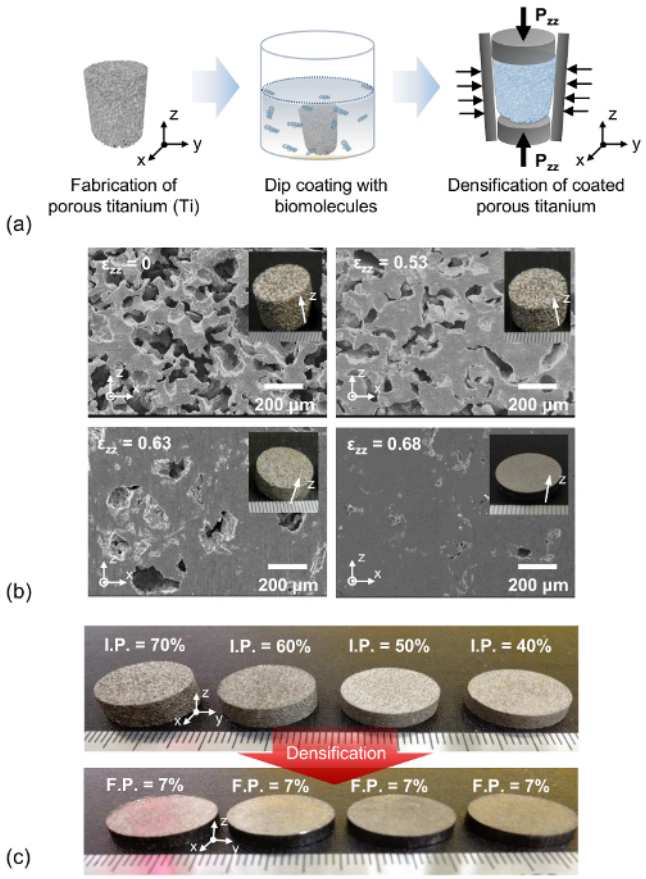

Figure 3. Dip-coating and densification of porous Ti scaffolds. (**A**) Schematic illustration of the fabrication process of a densified porous metallic scaffold (Ti) coated with biomolecules (*e.g.*, GFP) (Adapted with permission from Elsevier, Jung *et al.*, 2015). (**B**) Cross-section images of the densified porous Ti scaffolds (I.P. = 70%) at the applied strain (ε_{zz}) = 0, 0.53, 0.63, 0.68, resulting in the final porosity (F.P. = 70, 33, 19, 7%). (**C**) Optical images of the porous Ti specimens (I.P. = 70, 60, 50 and 40%) with various z-heights (top) and their corresponding densified specimens (F.P. = 7%) with the identical z-height of 2 mm after densification (bottom). Please click here to view a larger version of this figure.

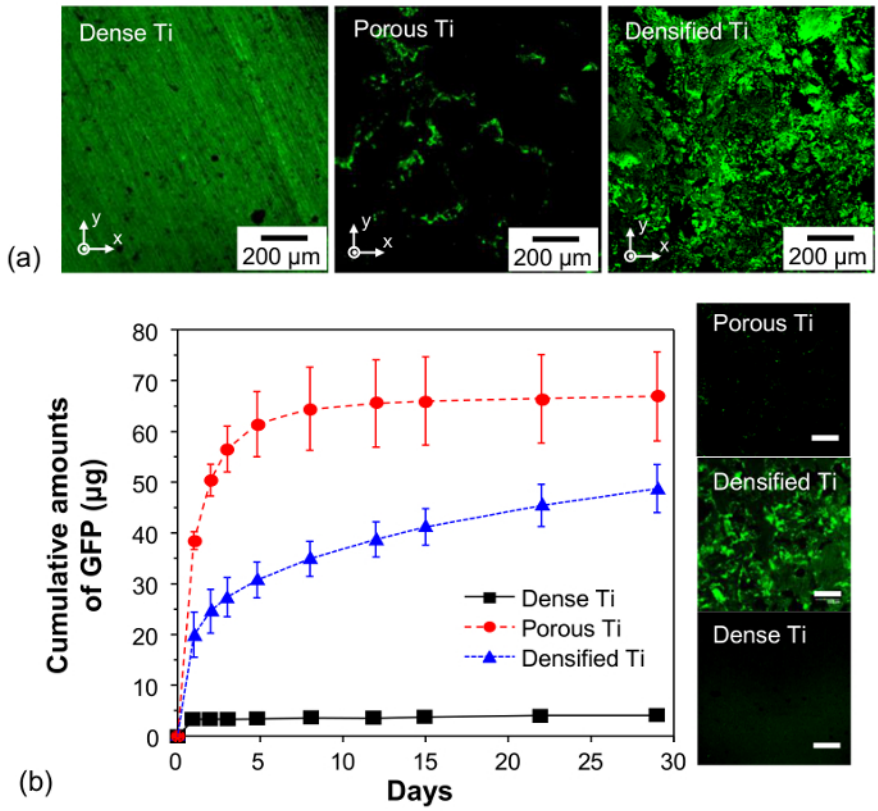

Figure 4. *In vitro* release behavior of GFP-loaded densified porous Ti scaffolds. (**A**) Typical CLSM images of GFP loaded on the surface of dense, porous and densified Ti scaffolds. (**B**) Cumulative amounts of GFP released from dense, porous and densified Ti scaffolds up to 29 days (n = 3) with the CLSM images of those three samples after immersion in the PBS for 24 days (scale bar = 200 μm). Standard deviation (SD) is used for the descriptive error bar of each data point. Please click here to view a larger version of this figure.

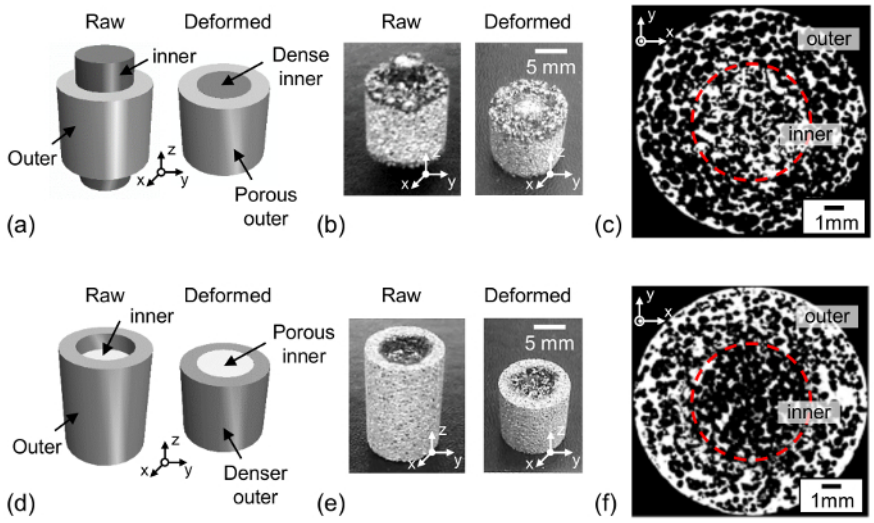

Figure 5. Fabrication of functionally graded porous metal scaffolds. (**A**) Schematic of a graded porous scaffold design with a denser inner part. (**B**) Graded porous Ti scaffold with the denser inner part fabricated through densification. (**C**) 2-D reconstructed micro-CT image of graded porous Ti scaffold with the denser inner part. (**D**) Schematic of a scaffold design with gradient porosity with the denser outer part. (**E**) Graded porous Ti scaffold with the denser outer part fabricated through densification in which the scaffold possesses a porous internal core surrounded by the densified outer layer. (**F**) 2-D reconstructed micro-CT image of graded porous Ti scaffold with the denser outer part. Please click here to view a larger version of this figure.

Target sample	Ti-camphene slurry			Coating solution	
	Ti powder (g)	Camphene (g)	KD-4 (g)	GFP (ml)	PBS (ml)
Ti scaffold with I.P. = 40%	204.3	90	0.294	1	9
Ti scaffold with I.P. = 50%	171.4	97	0.268		
Ti scaffold with I.P. = 60%	136.5	103	0.239		
Ti scaffold with I.P. = 70%	100	110	0.21		

Table 1. Detailed information of Ti-camphene slurry and coating solution for the fabrication of target porous Ti scaffolds (I.P. = 40, 50, 60, 70%) coated with GFP. (I.P. stands for initial porosity).

Initial porosity (%)	Final porosity (%)						
	60	50	40	30	20	10	5
50			0.17	0.29	0.38	0.44	0.47
60		0.20	0.33	0.43	0.50	0.56	0.58
70	0.25	0.40	0.50	0.57	0.63	0.67	0.68

Table 2. Predicted applied strain (ε_{zz}) of porous scaffolds (I.P. = 50, 60, 70%) in terms of the targeted final porosity (F.P.) using the equation, F.P. = 1 - (1- I.P.)/(1- ε_{zz}).

Specimen		Before densification			After densification		
		Height (mm)	Porosity (%)	Pore size (μm)	Height (mm)	Porosity (%)	Pore size (μm)
Graded scaffold of **Fig. 5b**	Inner part	18 ± 1	70 ± 1	370 ± 100	13 ± 1	57 ± 5	285 ± 100
	Outer part	14 ± 1				70 ± 5	365 ± 110
Graded scaffold of **Fig. 5e**	Inner part	14 ± 2			12 ± 1	70 ± 8	315 ± 110
	Outer part	18 ± 1				45 ± 8	230 ± 80

Table 3. Structural information of the inner and outer parts of graded porous scaffolds (Figure 5B and Figure 5E) before and after densification in terms of the z-height, porosity and average pore size measured by micro-CT.

Initial porosity of porous Ti (%)	Before densification		After densification (F.P.= 5%)	
	Stiffness (GPa)	Yield Strength (MPa)	Stiffness (GPa)	Yield Strength (MPa)
50	19	143	44	> 370
60	13	130	42	> 370
70	5	58	35	> 370

Table 4. Stiffness and yield strength of porous Ti scaffolds (I.P. = 50, 60, 70%) before and after densification (Adapted with permission from Elsevier, Jung *et al.*, 2015).

Discussion

While biometal systems have been widely used for biomedical applications, particularly, as load-bearing materials, high stiffness and low bioactivity of metals have been regarded as major challenges. In this study, we established the fabrication method of a new metal system, a densified porous metal scaffold which has biomimetic mechanical properties as well as bioactive surface with sustainable release behavior. The major advantages of our fabrication method include 1) no change in the previous dynamic freezing casting method which we already developed,[28] 2) control of one parameter-degree of densification-to achieve both the mechanical enhancement and sustainable release behavior of biomolecules from porous metal scaffolds and 3) potential application to functionally graded materials.

One of the critical steps needed to produce the densified porous metal is the fabrication of porous Ti, which possesses two important features: 1) ductility to control the release rate of bioactive molecules and the mechanical properties and 2) high pore interconnectivity to load and release biomolecules. However, previously reported porous titanium scaffolds produced using the space holder method, sponge template method, and powder metallurgy have shown either limited pore interconnectivity or ductility.[14,24,29] In particular, the impurities created by the reaction of metal powders with other surrounding materials during the heat treatment process are known to significantly reduce the ductility of the material because metal powders are in contact with the second materials (*e.g.*, space holder or polymer template), resulting in brittle failure under mechanical tests.[14,24,29] Thus, to fabricate densified porous metal, the impurities need to be minimized for most of the conventional fabrication

methods. To avoid this complication, we investigated the porous morphology and mechanical behaviors of porous titanium scaffolds fabricated using the freeze casting method with camphene in order to minimize the interaction between metal powders and the liquid phase.[26,28,30-33]

A disadvantage of the conventional freeze casting method is that it often results in directional pore channels (**Figure 2B**, top image). On the other hand, with dynamic freeze casting, the pore shape and size were found to be more uniform than those of the conventional freeze casting and the pore distribution within the scaffold is almost random. These structural features of porous scaffolds from dynamic freeze casting show isotropic mechanical behavior, thus allowing densification in a confined mold under uniaxial pressure.[26,28] During dynamic freeze casting, two major events occur within the metal slurry: 1) crystal growth of camphene phase and 2) redistribution of metal powders and solidified camphene within the remaining liquid phase avoiding sedimentation. Gravity causes the metal powders to segregate until the liquid camphene is fully solidified. The continuous rotation of the slurry near the melting temperature of camphene gives sufficient time for spherical camphene crystals to grow homogeneously, allowing the random and uniform distribution of Ti powders and camphene crystals as shown in **Figure 1C**.

Following the cooling process, fully solidified Ti-camphene biphasic green body (**Figure 1B**) was obtained. In order to completely remove the camphene from the solidified green body without the structure collapsing, camphene was sublimed in a vacuum desiccator at -20 °C. After removal of the camphene phase, the green body became porous, consisting of only Ti powder. Since there is no interaction among Ti particles, the porous Ti green body is fragile so that careful handling is required. To avoid any direct handling of the green body with hands before heat treatment, a ceramic crucible was chosen for the container of the green body for freeze-drying and sintering. The container with the green body was placed in a vacuum furnace immediately after the freeze-drying and heat treatment at 1,300 °C, which allows the green body to be fully densified without significant defects in the metal struts. For the evaluation of the samples, porous Ti blocks were cut into smaller porous Ti cylinders because the geometry and size of the porous samples should be identical (**Figure 2A**). All the specimens were successfully machined without any significant defects (**Figures 2B** and **2C**). Depending on the amount of Ti power in the slurry, Ti scaffolds with different porosities were obtained with spherical shapes and randomly distributed pores (**Figure 2C**).

After the porous Ti scaffolds were obtained using the dynamic freeze casting method as reported in our previous study,[28] the biomolecules were coated on the Ti surface and densification of the coated porous Ti was performed as illustrated in **Figure 3A**. In order to avoid any contamination or denaturation of the biomolecules, the coating process was conducted on a clean bench at RT within 24 hr after the porous scaffolds were autoclaved and carefully cleaned out. To minimize the loss of the coated biomolecules before densification, the cleaning process was minimized after the coating process was performed. The densification process was controlled by the applied deformation of the porous Ti samples in the z-direction, converted into strain, ε_{zz}.[26] Depending on the initial porosity of the Ti scaffolds, the applied strain and corresponding final porosity were varied (**Table 2**). In order to ensure the densified porous scaffolds with different initial porosities had identical final geometries and sizes, the applied strain of the individual scaffolds was calculated and the total sample height (length in z direction) of each sample was then predicted before densification. **Figure 3D** indicates that different heights of individual porous samples with varying porosity could lead to the densified porous sample with identical final height at the same final porosity.

By controlling the degree of densification, the densified porous scaffolds have unique mechanical behavior with prolonged release of the coated biomolecules. The applied strain changes two important parameters of the porous Ti scaffolds: final porosity and pore size. The porous scaffolds with lower porosity show higher stiffness and strength. Our previous study reported the stress-strain behavior of densified porous scaffolds with improved strength compared to porous Ti (**Table 4**) as well as significantly reduced stiffness compared to commercial dense Ti.[26] In this study, we also observed the release behavior of densified porous Ti compared with both dense and porous Ti through visualized detection of the GFP-coating layer as shown in **Figure 4**. The results were consistent with our previous study,[26] in which the densified porous scaffolds possess significantly improved release behavior of coated materials, prolonging the release time by up to four months due to increased torturosity of the scaffolds with decreased pore sizes. The current 30 day-release test clearly shows the remaining GFP on the surface of the densified porous Ti in contrast to no GFP remnant on either dense or porous Ti surfaces.

Finally, the densification method was applied to the production of functionally graded porous scaffolds in which the inner and outer parts have different porosities. For the cylindrical scaffold, differentiating the z-heights of the inner and outer parts can easily lead to graded porous scaffolds as shown in **Figure 5**. The applied strain (ε_{zz}) on the inner part in the porous Ti scaffold shown in **Figure 5B** was ~0.27, which resulted in the final porosity of ~ 57%, while no strain was applied to the outer part. On the other hand, the applied strain (ε_{zz}) on the outer part in the porous Ti scaffold in **Figure 5B** was ~0.33, which resulted in the final porosity of ~ 45% while the inner part was almost intact, preserving the initial porosity (**Table 3**). However, two major challenges for the graded porous scaffolds were observed from this experiment. First, the continuous inner and outer parts induced inconsistent stress and strain distribution within the scaffold; thus, the densification occurred inhomogeneously, where the regions around the top and bottom surfaces were denser than those around the inner surface. This tendency was critical as the height difference of the two parts increased. Moreover, the graded porous scaffold with the denser inner part was more difficult to produce than the scaffold with the denser outer part because the densification of the inner part should be carried out, being confined with the outer part, which resulted in inhomogeneous deformation within the two parts. To resolve the inhomogeneous densification of the graded scaffold, we developed two separate parts that can be assembled during the densification process. Even though in this paper, the optimal condition to produce the perfectly fabricated graded porous structure was not yet fully found, the potential of the densification process for the production of the graded structure was well confirmed. The optimized fabrication method of the graded porous structure is on-going, and as further work, selective drug loading to the graded structure will be investigated for the functional release behavior of the scaffold.

The advantages of the proposed approach in this study include 1) better mechanical compatibility with biological tissues with good strength and 2) prolonged bioactivity for better biological performance. However, one of the major disadvantages is the reduced pore size that cannot promote bone ingrowth through the pore network of metallic scaffolds for a better bone-implant interface. To resolve this issue, graded pore structures have been proposed, in which the porous and dense parts coexist; thus, the porous parts allow bone ingrowth, while the dense parts provide mechanical stability and prolonged bioactivity. Therefore, functionally graded Ti implants through various structural designs will be fabricated and tested, particularly, focusing on the improved capability of bone integration. Moreover, another limitation should be the fabrication of implants with complicated geometry. In order to obtain a complex-shaped implant (*e.g.*, femoral cone augment), the additional machining process is required after densification, imposing two major drawbacks on the final product: inefficient and uneconomical material usage because the significant volume of porous Ti block is often removed during the process, and potential contamination and loss of coated biomolecules during the machining process. Improvement on the fabrication process of the porous Ti scaffolds with complex geometry is ongoing. The densified

porous metal scaffolds can be applied to various orthopedic applications, *e.g.,* artificial disc replacement, replacing either bulk or porous metallic implants, and acting as a load support as well as a drug carrier.

Disclosures

The authors declare that they have no competing financial interests.

Acknowledgements

This research was supported by the Technology Innovation Program (Contract grant No. 0037915, WPM Biomedical Materials-Implant Materials) and Industrial Strategic Technology Development Program (Contract grant No. 10045329, Development of customized implant with porous structure for bone replacement), funded by the Ministry of Trade, industry & Energy (MI, Korea), and BK21 PLUS SNU Materials Division for Educating Creative Global Leaders (Contract grant No. 21A20131912052).

References

1. Long, M., Rack, H. Titanium alloys in total joint replacement-a materials science perspective. *Biomaterials.* **19** (18), 1621-1639 (1998).
2. Niinomi, M. Recent metallic materials for biomedical applications. *Metall. Mater. Trans. A.* **33** (3), 477-486 (2002).
3. Frosch, K. H., Stürmer, K. M. Metallic biomaterials in skeletal repair. *Eur. J. Trauma.* **32** (2), 149-159 (2006).
4. Huiskes, R., Weinans, H., Van Rietbergen, B. The relationship between stress shielding and bone resorption around total hip stems and the effects of flexible materials. *Clin. Orthop. Relat. Res.* **274**, 124-134 (1992).
5. Kanayama, M., *et al. In vitro* biomechanical investigation of the stability and stress-shielding effect of lumbar interbody fusion devices. *J. Neurosurg. Spine.* **93** (2), 259-265 (2000).
6. Jung, H.-D., Kim, H.-E., Koh, Y.-H. Production and evaluation of porous titanium scaffolds with 3-dimensional periodic macrochannels coated with microporous TiO_2 layer. *Mater. Chem. Phys.* **135**, 897-902 (2012).
7. Jones, A.C., *et al.* Assessment of bone ingrowth into porous biomaterials using MICRO-CT. *Biomaterials.* **28** (15), 2491-2504 (2007).
8. Li, J. P. *et al.* Bone ingrowth in porous titanium implants produced by 3D fiber deposition. *Biomaterials.* **28** (18), 2810-2820 (2007).
9. Ahn, M.-K., Jo, I.-H., Koh, Y.-H., Kim, H.-E. Production of highly porous titanium (Ti) scaffolds by vacuum-assisted foaming of titanium hydride (TiH_2) suspension. *Mater. Lett.* **120** (1), 228-231 (2014).
10. Baas, J., *et al.* The effect of pretreating morselized allograft bone with rhBMP-2 and/or pamidronate on the fixation of porous Ti and HA-coated implants. *Biomaterials.* **29** (19), 2915-2922 (2008).
11. Peng, L., Bian, W.-G., Liang, F.-H., Xu, H.-Z. Implanting hydroxyapatite-coated porous titanium with bone morphogenetic protein-2 and hyaluronic acid into distal femoral metaphysis of rabbits. *Chin. J. Traumatol. (English Edition).* **11** (3), 179-185 (2008).
12. Reiner, T., Kababya, S., Gotman, I. Protein incorporation within Ti scaffold for bone ingrowth using Sol-gel SiO_2 as a slow release carrier. *J. Mater. Sci. - Mater. Med.* **19**, 583-589 (2008).
13. Lee, J.H., Kim, H.E., Shin, K.H., Koh, Y.H. Improving the strength and biocompatibility of porous titanium scaffolds by creating elongated pores coated with a bioactive, nanoporous TiO_2 layer. *Mater. Lett.* **64**, 2526-2529 (2010).
14. Li, J.C., Dunand, D.C. Mechanical properties of directionally freeze-cast titanium foams. *Acta Mater.* **59** (1), 146-158 (2011).
15. Chino Y., Dunand, D.C. Directionally freeze-cast titanium foam with aligned, elongated pores. *Acta Mater.* **56** (1), 105-113 (2008).
16. Kim, S.W., *et al.* Fabrication of porous titanium scaffold with controlled porous structure and net-shape using magnesium as spacer. *Mater. Sci. Eng. C.* **33** (5), 2808-2815 (2013).
17. Brentel, A.S. *et al.* Histomorphometric analysis of pure titanium implants with porous surface versus rough surface. *J. Appl. Oral Sci.* **14** (3), 213-218 (2006).
18. Buser, D. *et al.* Influence of surface characteristics on bone integration of titanium implants. A histomorphometric study in miniature pigs. *J. Biomed. Mater. Res.* **25** (7), 889-902 (1991).
19. Cochran, D., Schenk, R., Lussi, A., Higginbottom, F., Buser, D. Bone response to unloaded and loaded titanium implants with a sandblasted and acid-etched surface: a histometric study in the canine mandible. *J. Biomed. Mater. Res.* **40** (1), 1-11 (1998).
20. Young, D.R., Robb, R.A., Rock, M.G., Chao, E.Y. Analysis of periprosthetic tissue formation around a porous titanium endoprosthesis using CT-based spatial reconstruction. *J. Comput. Assist. Tomo.* **18** (3), 461-468 (1994).
21. Spoerke, E.D., *et al.* A bioactive titanium foam scaffold for bone repair. *Acta Biomater.* **1** (5), 523-533 (2005).
22. Jung, H. D. *et al.* Highly aligned porous Ti scaffold coated with bone morphogenetic protein-loaded silica/chitosan hybrid for enhanced bone regeneration. *J. Biomed. Mater. Res. Part B Appl. Biomater.* **102** (5), 913-921 (2013).
23. Ryan, G. E., Pandit, A. S., Apatsidis, D. P. Porous titanium scaffolds fabricated using a rapid prototyping and powder metallurgy technique. *Biomaterials.* **29** (27), 3625-3635 (2008).
24. Vasconcellos, L.M.R., *et al.* Porous titanium scaffolds produced by powder metallurgy for biomedical applications. *Mater.* Res. **11** (3), 275-280 (2008).
25. Jung, H.D., Yook, S.W., Kim, H.E., Koh, Y.H. Fabrication of titanium scaffolds with porosity and pore size gradients by sequential freeze casting. *Mater. Lett.* **63** (17), 1545-1547 (2009).
26. Jung, H.-D., Jang, T.-S., Wang, L., Kim, H.-E., Koh, Y.-H., Song, J. Novel strategy for mechanically tunable and bioactive metal implants. *Biomaterials.* **37**, 49-61 (2015).
27. Tarng, Y.S., Ma, S.C., Chung, L.K. Determination of optimal cutting parameters in wire electrical discharge machining. *Int. J. Mach. Tools Manufact.* **35** (12), 1693-1701 (1995).
28. Jung, H.-D., *et al.* Dynamic Freeze Casting for the Production of Porous Titanium (Ti) Scaffolds. *Mater. Sci. Eng. C.* **33** (1), 59-63 (2013).
29. Lee, J.-H., Kim, H.-E., Shin, K.-H., Koh, Y.-H. Improving the strength and biocompatibility of porous titanium scaffolds by creating elongated pores coated with a bioactive, nanoporous TiO_2 layer. *Mater. Lett.* **64** (22), 2526-2529 (2010).
30. Jung, H.-D., Yook, S.-W., Kim, H.-E., Koh, Y.-H. Fabrication of titanium scaffolds with porosity and pore size gradients by sequential freeze casting. *Mater. Lett.* **63** (17), 1545-1547 (2009).

31. Yook, S.-W. *et al.* Reverse freeze casting: A new method for fabricating highly porous titanium scaffolds with aligned large pores. *Acta Biomater.* **8** (6), 2401-2410 (2012).
32. Yook, S.W., Yoon, B.H., Kim, H.E., Koh, Y.H., Kim, Y.S. Porous titanium (Ti) scaffolds by freezing TiH_2/camphene slurries. *Mater. Lett.* **62** (30), 4506-4508 (2008).
33. Yook, S.W., Kim, H.E., Koh, Y.H. Fabrication of porous titanium scaffolds with high compressive strength using camphene-based freeze casting. *Mater. Lett.* **63** (17), 1502-1504 (2009).

